Ultrafast Dynamics of Metal Complexes of Tetrasulphonated Phthalocyanines

Arkadiusz Jarota, Marc Tondusson, Geoffrey Galle, Eric Freysz, Halina Abramczyk

Ultrafast Dynamics of Metal Complexes of Tetrasulphonated Phthalocyanines

Arkadiusz Jarota,[†] Marc Tondusson,[‡] Geoffrey Galle,[‡] Eric Freysz,[‡] and Halina Abramczyk*,[†]

[†]Institute of Applied Radiation Chemistry, Laboratory of Laser Molecular Spectroscopy, Technical University of Lodz, Wroblewskiego 15, 93 590 Lodz, Poland

[‡]Laboratoire Ondes et Matière d'Aquitaine (LOMA), Université Bordeaux 1, UMR CNRS 5798, 351 Cours de la Libération 33405 Talence Cedex, France

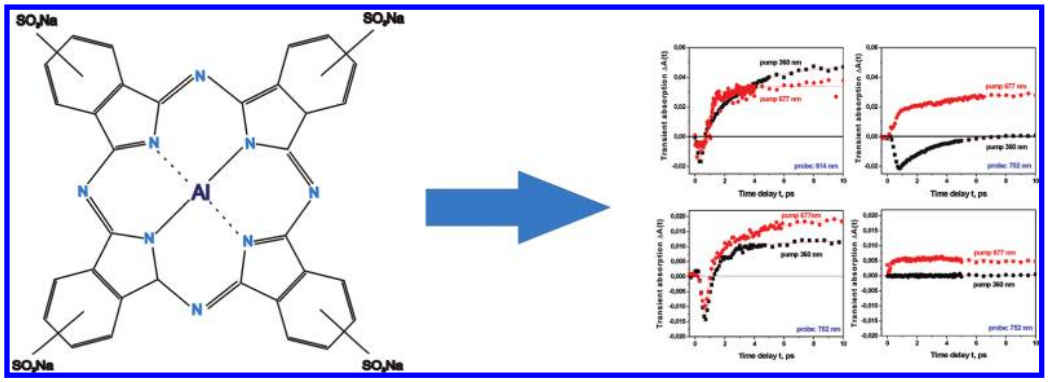

ABSTRACT: A promising material in medicine, electronics, optoelectronics, electrochemistry, catalysis, and photophysics, tetrasulphonated aluminum phthalocyanine ($AlPcS_4$), is investigated by means of steady state and time resolved pump−probe spectroscopies. Absorption and steady state fluorescence spectroscopy indicate that $AlPcS_4$ is essentially monomeric. Spectrally resolved pump−probe data are recorded on time scales ranging from femtoseconds to nanoseconds. The nature of these fast processes and pathways of the competing relaxation processes from the initially excited electronic states in aqueous and organic (dimethyl sulfoxide) solutions are discussed. The decays and bleaching recovery have been fitted in the ultrafast window (0−10 ps) and later time window extending to nanoseconds (0−1 ns). While the excited state dynamics have been found to be sensitive to the solvent environment, we were able to show that the fast dynamics is described by three time constants in the ranges of 115−500 fs, 2−25 ps, and 150−500 ps. We were able to ascribe these three time constants to different processes. The shortest time constants have been assigned to vibrational wavepacket dynamics. The few picosecond components have been assigned to vibrational relaxation in the excited electronic states. Finally, the 150−500 ps components represent the decay from S_1 to the ground state. The experimental and theoretical treatment proposed in this paper provides a basis for a substantial revision of the commonly accepted interpretation of the Soret transition (B transition) that exists in the literature.

INTRODUCTION

Phthlocyanines and metallophthalocyanines are involved in many biological, chemical, and physical processes. The pos sibility to tailor and modify their properties such as absorption, emission, nonlinear optical responses, polarizability, and dipole moment make them extremely important materials in many disciplines of research like biomedicine, electronics, optoelec tronics, electrochemistry, photophysics, and catalysis. The diversity of their functions is due in part to the variety of metals that bind in the "pocket" of the phthalocyanine ring system. They have been proven to be efficient photosensitizers in a number of chemical and photochemical processes, especially photodynamic therapy (PDT).

PDT of cancer is a promising application, particularly for small and superficial tumors as well as benign skin and mouth disorders. At present, PDT is also being tested in the clinic for use to treat cancers of the brain, head and neck, lung, pancreas, intraperitoneal cavity, skin, prostate, and breast.[1−8] Recently, the targeted PDT technique has been tested on breast cancer cells.[9−11] aluminum tetrasulphonated phthalocyanine ($AlPcS_4$) has been used in clinical trials[12−14] because its triplet state has the ability to react with molecular oxygen to produce highly reactive singlet oxygen. Despite the medical applications, a growing numbers of phthalocyanines play an important role as low gap semiconducting materials.[15]

The processes of energy dissipation in phthalocyanines occurring on the nanosecond time scale, such as internal con version, fluorescence, intersystem crossing, and the triplet forma tion, have been studied in many papers.[16−35] There are many fewer papers reporting on primary events in phthalocyanines

occurring on femtosecond and picosecond scales,[23,36−43] which are particularly important in thin films. The effects of aggre gation on the absorption and emission spectra of metalloph thalocyanines in the liquid solutions are well documented[44−53] but much less information has been accumulated on the solid phases. The films of phthalocyanines become relevant in advanced devices like electrochromic displays, optical limiters, light emitting diodes, recordable digital discs, organic conductors, lasers, nonlinear optical elements, and so forth. In these applications, properties such as conductivity, optical absorbance, and photoconductivity in the solid state phase are important.[15,54]

In this paper, $AlPcS_4$ has been chosen to serve as a model phothosenistizer to study the efficiency of primary processes occurring upon excitation of the chromophore that lead to the triplet generation.

In this paper, we wish to elucidate processes responsible for fast dynamics of $AlPcS_4$ occurring on the time scale from femtoseconds to nanoseconds monitored by the pump−probe transient absorption spectroscopy when induced by femto second laser pulses centered at 677 and 360 nm, corresponding to the absorption maxima of the Soret band and the Q band, respectively.

EXPERIMENTAL SECTION

Aluminum phthalocyanine chloride tetrasulphonic acid was purchased from Frontier Scientific, Inc. (AlPcS 834). Dimethyl sulfoxide (DMSO) was purchased from Sigma Aldrich (34869). They were used without further purification. Water was deionized before preparing the solutions. Briefly, Scheme 1 illustrates the

Scheme 1. Method Used for Synthesis of $AlPcS_4$ via Sulphonation of the Non Sulphonated Phthalocyanine

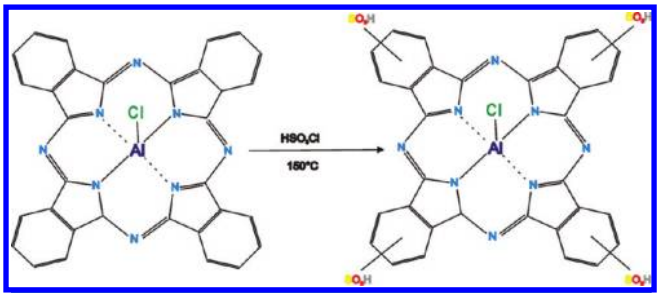

method used for synthesis of $AlPcS_4$ via sulphonation of the nonsulphonated phthalocyanine. This method leads to a large number of regioisomers.

Steady-State Emission Measurements. Emission spectra were measured with a Ramanor U1000 (Jobin Yvon) and Spectra Physics 2017 04S argon ion laser operating at 514 nm at a power of 100 mW. The spectral slit width was 6 cm^{-1}, which corresponds to the 500 μm mechanical slit of the spectrometer; a $\lambda/4$ wave plate was used to change the linear polarization into the circular one to avoid the different polar ization sensitivity of the gratings. The interference filter has been used to purify the laser line by removing additional natural emission lines that interfere with the Raman lines, especially in the case of the solid samples.

Steady-State UV−Vis Absorption Measurements. UV−vis absorption electronic spectra were measured with Varian Cary 5E spectrophotometer in 2 and 0.10 ± 0.005 mm detachable quartz cells (Hellma). The spectra were recorded at 293 K for the aqueous solutions and in DMSO at con centrations of $c = 10^{-5}$, 10^{-4}, and 10^{-3} M.

Pump−Probe Transient Absorption Spectroscopy. The source of the femtosecond pulses was a mode locked titanium sapphire femtosecond laser (MIRA, Coherent, 800 nm, 76 MHz, 9 nJ, <200 fs) pumped with a diode pumped solid state laser (VERDI V5, Coherent, 532 nm). The fundamental beam was amplified with a Ti:Sapphire regenerative amplifier (Coherent Legend USP, 800 nm, 1 kHz, 3 mJ, 50 fs). The regenerative amplifier was pumped with a diode pumped Nd:YLF laser (JADE, Thales Laser, 527 nm, 1 kHz, 20 mJ, <200 ns). The pulse was split in two and further amplified in a dual single pass amplifier (Coherent Elite Duo, 800 nm, 1 kHz, 2 × 4.5 mJ, 50 fs). This amplifier was pumped by a high power Nd:YLF laser (Evolution, Coherent, 527 nm, 50 mJ, <200 ns). The output of the laser system was split, and two 1 mJ laser pulses were used to pump two optical parametric amplifiers (OPA, model TOPAS from Light Conversion). These OPA combined by frequency conversion modules generate femto second pulses tunable in the 300 and 2600 nm ranges. The energy of the pump pulse was adjusted to 2 μJ in water experiments and 700 nJ or less in experiments with DMSO. The energy of the probe pulse was at least 100 times lower than the energy of the pump pulse. The pump and probe pulses were overlapped on a 1 mm optical path of a cell containing the $AlPcS_4$ solution. The solution was circulated in the cell by a magnetic stirrer in order to minimize the thermal lensing and photoquenching effects. The time delay t between the pump and probe pulses was adjusted by a motorized translation stage that has a spatial resolution of 1.5 μm. Transient absorption signals was measured with two silicon photodiodes (Thorlabs, TDS 1000) placed before and after the sample, which measure initial (I_0) and the transmitted intensity of the probe beam (I_t) respectively. The I_0 was normalized with respect to the intensity of the pump beam, which was measured with the same type of the photodiode. The absorption signal $S(t)$ was calculated as $\log(I_0/I_t)$ The transient absorption signal $\Delta A(t)$ was computed by subtracting the absorption signal measured with and with out the pump pulse. For that reason, the pump beam was chopped at 40 Hz. The typical measurement error of ΔA was better than 10^{-3}.

Computational Method. Geometry optimizations have been performed using Gaussian 03 software[55] on the DFT level with the B3LYP hybrid functional and 6 31G(d) basis set. Additionally, to get more insight into electronic transitions, we have carried out the TD DFT calculations at the B3LYP 6 31G(d) level.

RESULTS

Steady-State Absorption and Emission Measurements. The steady state absorption spectra of $AlPcS_4$ in water and DMSO as a function of concentration are shown in Figure 1. The Q band ($S_0(a_{2u}) \rightarrow S_1(e_g)$ transition) has a sharp maximum at 678 nm as well as weaker bands to the blue side with maxima at 643 and 607 nm. The shape, the positions of the absorption maxima, and the intensity of the bands at 643, 607, and at 678 nm are normalized to the maximum of the band at 678 nm. One can see that the absorption bands are very similar in the concentration range of 10^{-5}−10^{-3} M, indicating that $AlPcS_4$ molecules are dominated by a monomeric form in both solvents.

The fluorescence spectrum presented in Figure 2 (λ_{exc} = 514 nm) shows an almost perfect mirror image of the absorption spectrum in the Q band region, indicating that the bands at 643 and 607 nm should be assigned to the vibrational progression.

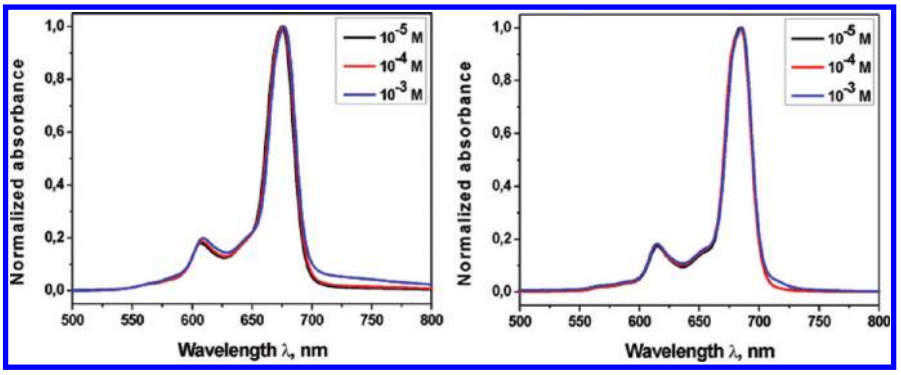

Figure 1. Normalized absorption spectra of $AlPcS_4$ solutions in the concentration range of 10^{-5}–10^{-3} M, (a) in water and (b) in DMSO.

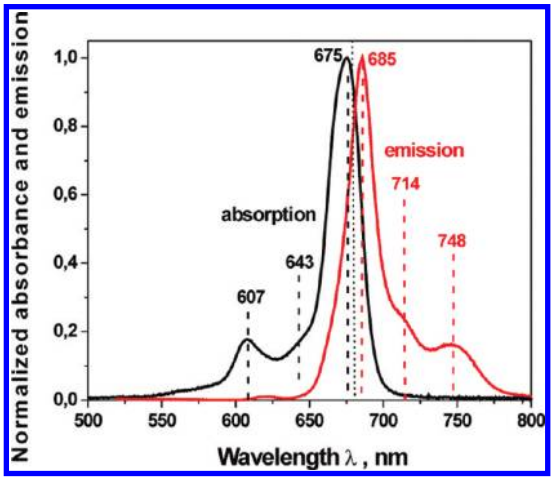

Figure 2. Normalized absorption and emission spectra of $AlPcS_4$ in aqueous solution at a concentration of $c = 10^{-6}$ M.

The maximum of emission at 685 nm provides a Stokes shift of 8 nm. However, at higher concentrations, the fluorescence spectrum presented in Figure 3 (λ_{exc} = 514 nm) shows no

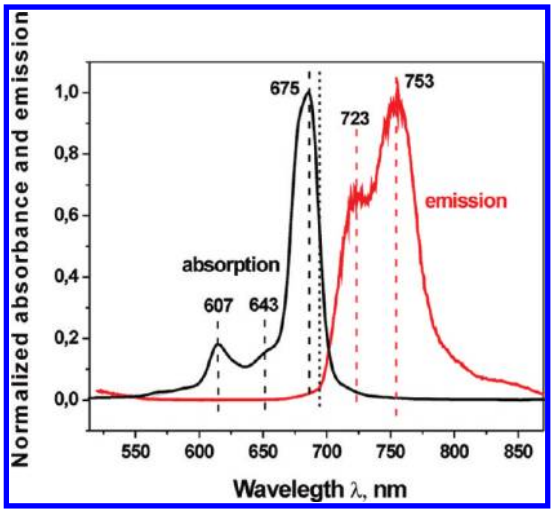

Figure 3. Normalized absorption and emission spectra of $AlPcS_4$ in aqueous solution at a concentration of $c = 10^{-3}$ M.

features of the mirror image of the absorption and the emission spectra in the Q band region, indicating that the contribution from reabsorption and aggregation leads to disturbance of the image typical for the monomeric form.

The absorption at high concentrations becomes solvent dependent. Figure 4 shows the absorption of $AlPcS_4$ at $c = 10^{-3}$

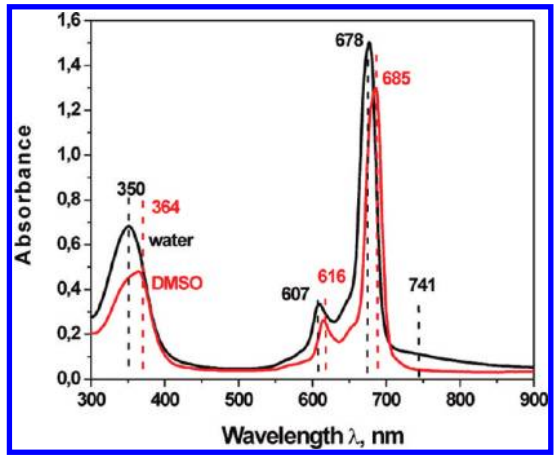

Figure 4. Absorption spectra of $AlPcS_4$ solution in water (black line) and in DMSO (red line) for $c = 10^{-3}$ M; optical length = 0.1 mm.

M in DMSO and water. The band in DMSO is red shifted from 678 to 685 nm and is substantially narrowed relative to the absorption bands in water. The red shift in organic solvents has been attributed to a shift from aggregates toward monomers.[56,57] The results from Figure 4 indicate that the $AlPcS_4$ molecules are more aggregated in water, while in DMSO, they are almost monomeric even at high concentrations.

Figure 5 shows the emission of $AlPcS_4$ at $c = 10^{-5}$ and 10^{-3} M in DMSO and water. The emission spectra are much more concentration sensitive, particularly at high concentrations. The distinctions observed in the emission spectra at higher concentrations must be related to different paths of energy dissipation.

Excited-State Dynamics of $AlPcS_4$ in Aqueous and DMSO Solutions. *$S_0(a_{1u}) \rightarrow S_1(e_g)$ Transition.* To get a deeper insight into the mechanisms of energy dissipation in phthalocyanines, we have monitored the excited state dynamics in aqueous and organic (DMSO) solvents upon excitation at 677 nm, which promotes the $S_0(a_{1u}) \rightarrow S_1(e_g)$ transition in the Q band (Scheme 2).

Figure 6 shows the transient absorption signals $\Delta A(t)$ of $AlPcS_4$ in aqueous and organic (DMSO) solvents at a concentration of 10^{-3} M as a function of the time delay t in the pump–probe experiments. The molecules were excited at 677 nm and probed at different wavelengths (500, 572, 664, and 690 nm). The right panel shows the results in DMSO, and the left panel

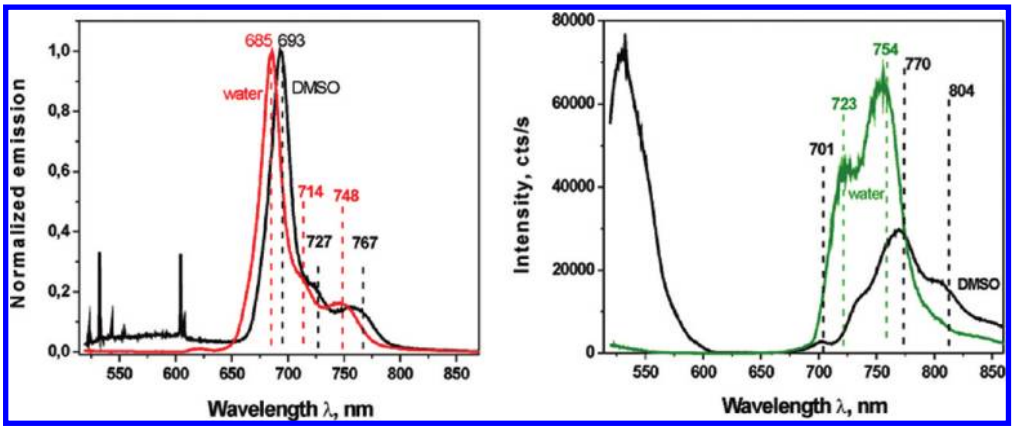

Figure 5. Emission spectra of $AlPcS_4$ in DMSO and in water at c = (a) 10^{-5} and (b) 10^{-3} M.

Scheme 2. Excitation of the Excited Electronic States Pumped with the Pulses at 360 and 677 nm

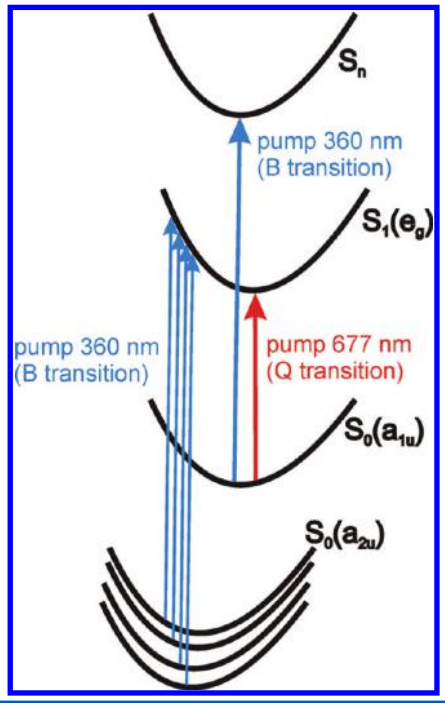

shows the results in aqueous solution. The results in Figure 6 are presented in the full time window up to 1 ns.

Comparison between Figure 6a and b demonstrates that in DMSO, the excited state dynamics of $AlPcS_4$ is drastically different from that in water. Directly upon excitation with the laser pump pulse at 677 nm, a negative signal at 664 nm (Figure 6a) has been recorded in the aqueous solution of $AlPcS_4$. The latter phenomenon is assigned to the bleaching of the Q transition. The bleach is instantaneous and is laser pulse width limited. In water, the recovery of the bleach at 664 nm is found to be biexponential and is fitted with time constants of 5.09 ± 0.99 and 203.16 ± 18.75 ps. It is important to notice that the recovery goes above the baseline at around 400 ps and the signal becomes positive. The time constants are of the same order as those obtained by Howe et al.[23] for PcS_4 and $ZnPcS_4$ in DMSO probed at 720, 790, and 820 nm. Even though we slightly shifted the probe wavelength, one can observe the bleaching in water (Figure 6a) but no evidence of bleaching in DMSO (Figure 6b). In DMSO, we recorded a sudden rise instead.

Figure 6a shows that the instantaneous bleach of $AlPcS_4$ in water at 664 nm is accompanied by a sudden rise at 500 nm that is followed by decay. This decay is found to be biexponential and is fitted with time constants of 3.23 ± 0.68 and 304 ± 39 ps in water (Figure 6a) and 24 ± 19 and 380 ± 178 ps in DMSO (Figure 6b).

Further ultrafast dynamics can be monitored in other regions of the transient absorption spectrum (572 nm in Figure 6a,b). The sudden rise at 572 nm is followed by a decay that is found to be biexponential and that is fitted with time constants of 3.51 ± 0.50 and 220 ± 25 ps in water and 3.44 and 115 ± 95 ps in

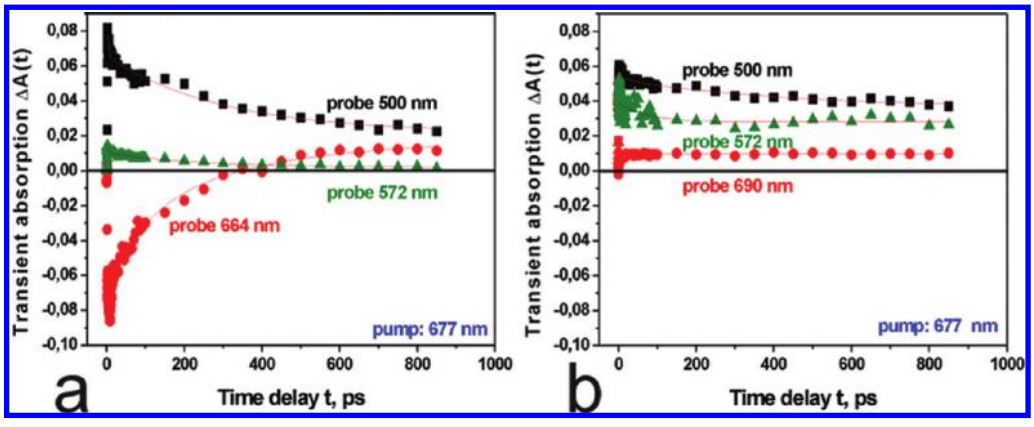

Figure 6. Transient absorption signal $\Delta A(t)$ of $AlPcS_4$ in water (a) and DMSO (b) as a function time delay in the full time window up to 1 ns, pumped at 677 nm and probed at 500, 572, 664, and 690 nm; concentration = 10^{-3} M.

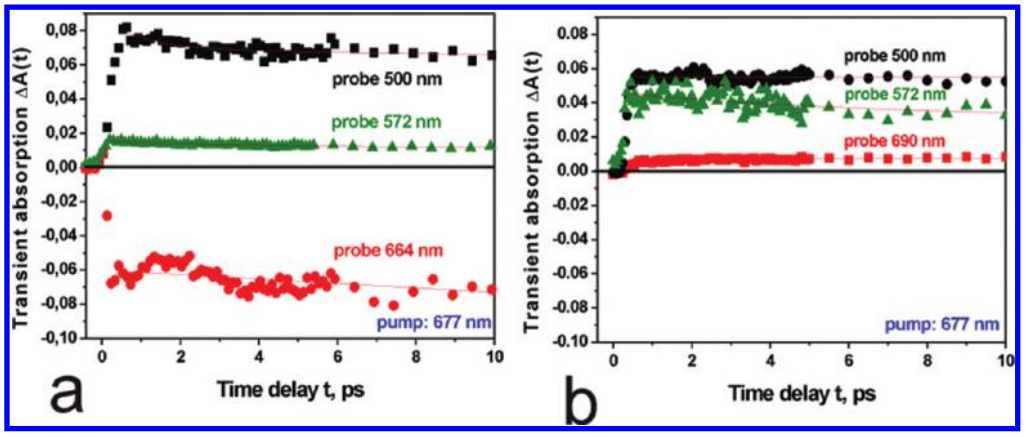

Figure 7. Transient absorption signal $\Delta A(t)$ of $AlPcS_4$ in water (a) and DMSO (b) as a function of time delay in the early time window up to 10 ps, pumped at 677 and probed at 500, 572, 664, and 690 nm; concentration = 10^{-3} M.

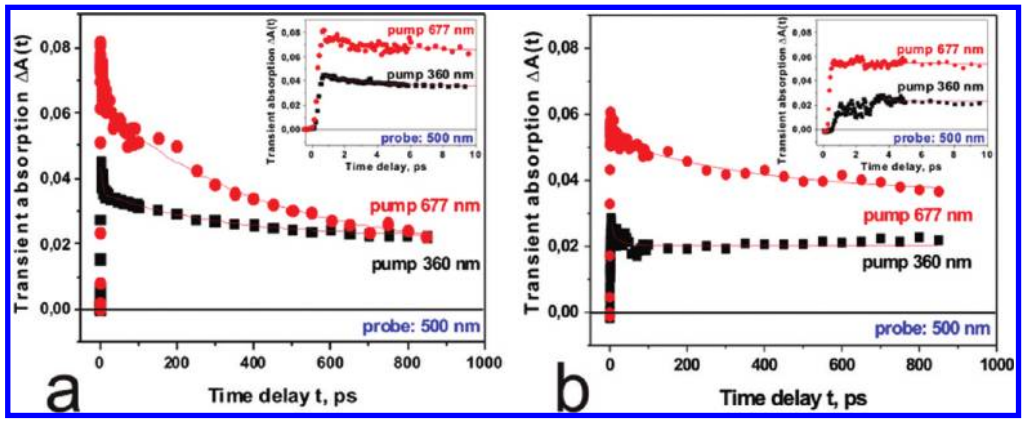

Figure 8. Transient absorption signal $\Delta A(t)$ of $AlPcS_4$ in water (a) and DMSO (b) as a function time delay in the full time window up to 1 ns, probed at 500 nm, pumped at 677 and 360 nm; concentration = 10^{-3} M. The insets show the signal $\Delta A(t)$ in the time window up to 10 ps.

DMSO, indicating that the signals observed in the range of 500−572 nm demonstrate similar features of dynamics.

Figure 7 presents the results for $AlPcS_4$ in water (Figure 7a) and in DMSO (Figure 7b) in the early time window extending to 10 ps. The initial decays of the signal at 500 nm are monoexponential and can be fitted with a time constant of 244 ± 98 fs in water and 155 ± 51 fs in DMSO. The decays of the signal at 572 nm are monoexponential and can be fitted with a time constant of 560 ± 94 fs in water and 480 ± 384 fs in DMSO. Savolainen and co workers[39] have studied ZnPc in DMSO (0.12×10^{-3} M). They obtained three time constants, 250 fs, 2.5 ps, and 2.9 ns. Bearing in mind that the study in ref 39 was on ZnPc, not $AlPcS_4$, we nonetheless feel that a com parison is worthwhile. We find no evidence of the slow com ponent (2.9 ns) in our measurements of the transient absorption. The slowest component of dynamics of the order 150−500 ps observed in our paper at different wavelengths is similar to that reported by Howe et al.[23] On the other side, we find that the fast, femtosecond components obtained in this paper, which were demonstrated by the time constant of 244 (in water) and 155 fs (in DMSO) for the 500 nm and of 560 fs (480 fs) in water (DMSO) for 572 nm probing wavelengths, are similar to the time constants reported by Savolainen et al.[39]

$S_0(a_{2u}) \rightarrow S_1(e_g)$ Transition. The pumping at 360 nm excites the transition $S_0(a_{2u}) \rightarrow S_1(e_g)$ and/or the S_n state (Scheme 2). Figure 8 compares the transient absorption signals $\Delta A(t)$ recorded at 500 nm when the sample is pumped at 677 and 360 nm. In water, the instantaneous rise at 500 nm, limited by the laser pulse duration, is followed by a biexponential decay with time constants of 3.23 ± 0.68 and 304 ± 39 ps for the pumping at 677 nm and 3.18 ± 0.19 and 299.38 ± 24 ps for the pumping at 360 nm. In DMSO, the relevant time constants are 24 ± 19 and 380 ± 17 ps for pumping at 677 nm and 24.06 ± 9.57 and 220 ± 180 fs for pumping at 360 nm. Thus, both components of the dynamics are similar for both pumping wavelengths in both solvents.

Figure 9 compares the transient absorption signals $\Delta A(t)$ of $AlPcS_4$ at the probe wavelength of 572 nm in water (left panel) and in DMSO (right panel) when the sample is pumped at 360 and 677 nm, respectively. In water, when the sample is pumped at 360 nm, the decay of the positive signal of $AlPcS_4$ at 572 nm is found to be biexponential and is fitted with time constants of 58 ± 24 and 614 ± 378 ps. However, when the sample is pumped at 677 nm, the decay of the signal is found to be biexponential and fitted with time constants of 3.51 ± 0.50 and 220 ± 25 ps. In DMSO, the decay of positive signals of $AlPcS_4$ at 572 nm is found to be biexponential and is fitted with time constants of 3.44 ± 1.31 and 115 ± 81 ps and 2.00 ± 0.13 and 360 ± 152 ps when the sample is pumped at 667 and 360 nm, respectively. As the positive signals at 500 and 572 nm in Figures 8 and 9 appear instantaneously within the femtosecond time scale, we have assigned them to the excited state absorption (ESA).

Figure 10 compares the transient absorption signals $\Delta A(t)$ of the sample pumped at 360 and 677 nm and probed at wavelengths of 614 and 752 nm when $AlPcS_4$ is dissolved in water and 702 and 752 nm when $AlPcS_4$ is dissolved in DMSO. In water, directly upon excitation, instantaneous bleach (negative

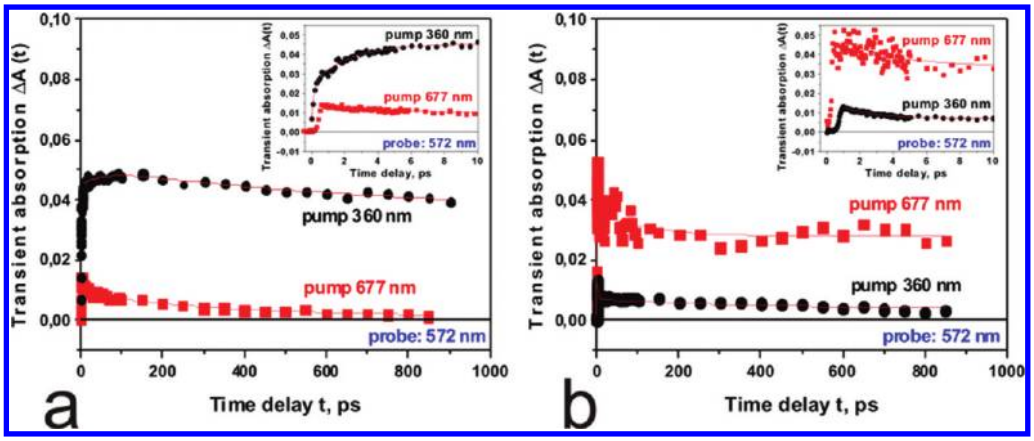

Figure 9. Transient absorption signal $\Delta A(t)$ of $AlPcS_4$ at the probe wavelength of 572 nm in water (a) and in DMSO (b) for pumping at 360 and 677 nm; concentration = 10^{-3} M. The insets show the signal $\Delta A(t)$ in the time window up to 10 ps.

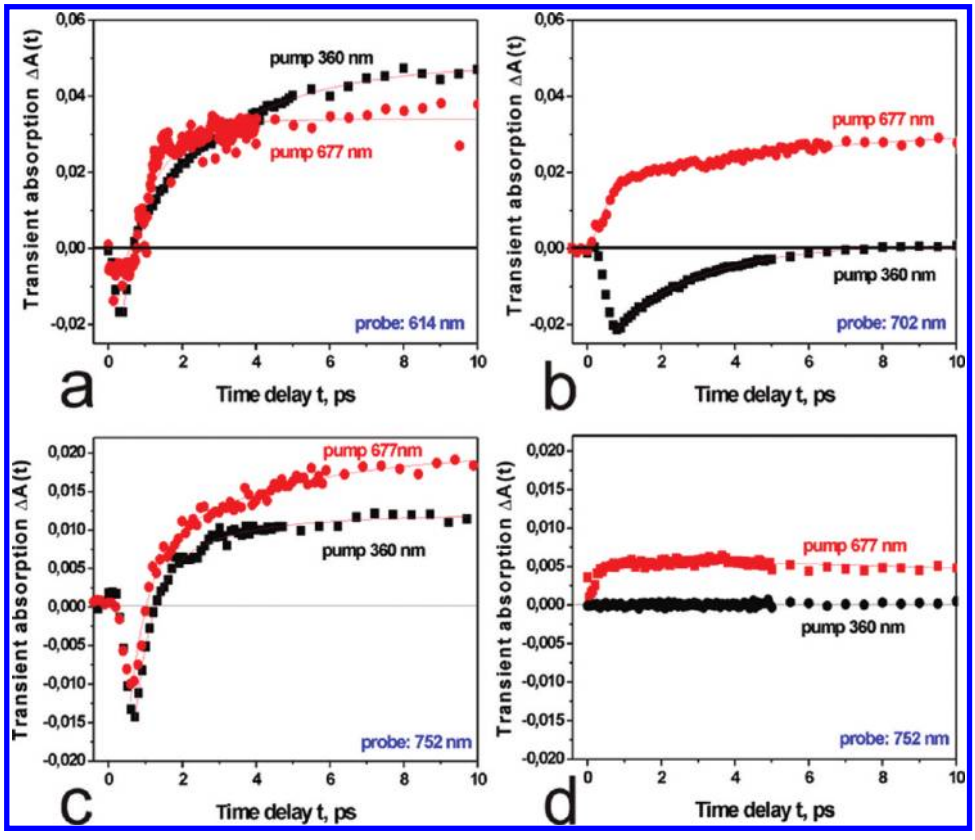

Figure 10. Transient absorption signal $\Delta A(t)$ of $AlPcS_4$ in water (a,c) and DMSO (b,d) as a function time delay in the early time window up to 10 ps, pumped at 360 and 677 nm and probed at 614, 702, and 752 nm; concentration = 10^{-3} M.

signal) is present at 614 and 752 nm. This instantaneous bleach (laser pulse width limited) is followed by a recovery. The recovery of the bleach at 614 nm, when the sample is pumped at 360 nm, is found to be biexponential and is fitted with time constants of 231 ± 26 fs and 2.75 ± 0.10 ps in the early window up to10 ps. In water, when the sample is probed at 752 nm, the recovery of the bleach is found to be biexponential and is fitted with time constants of 490 ± 70 fs and 3.79 ± 1.25 ps for pumping at 677 nm and 480 ± 60 fs and 2.33 ± 0.81 ps for pumping with 360 nm. In DMSO, the bleaching is observed only for pumping at 360 nm. When the probe is set at 702 nm, the bleaching is fitted by a biexponential function with time constants of 450 ± 302 fs and 2.45 ± 10 ps. Contrary, when the sample is pumped at 677 nm and probed at 702 nm, one records a positive signal. Its rise is found to be fitted by a biexponential function with the time constants of 460 ± 60 fs and 6.12 ± 2.12 ps. For all of the signals presented in Figure 10, it is important to notice that the recovery signals at 614, 702, and 752 nm go above the baseline at around 400 ps, and the signal becomes positive. For the probe wavelength at 752 nm, the difference in the signal in water and that in DMSO presented in Figure 10c and d is most likely due to a coincidental cancellation between the bleach and ESA ($S_1 \rightarrow S_n$).

DISCUSSION

In order to elucidate further electronic dynamics features that can be rationalized from the signals of the transient absorption

Scheme 3. Energy Level Diagrams for Selected Metal Complexes of Phthalocyanines (a) ZnPc,[58,60] (b) Various Complexes of Phthalocyanines,[59] (c) ZnPc,[39] (d) $AlPcS_4$ from TD DFT Calculations in This Paper

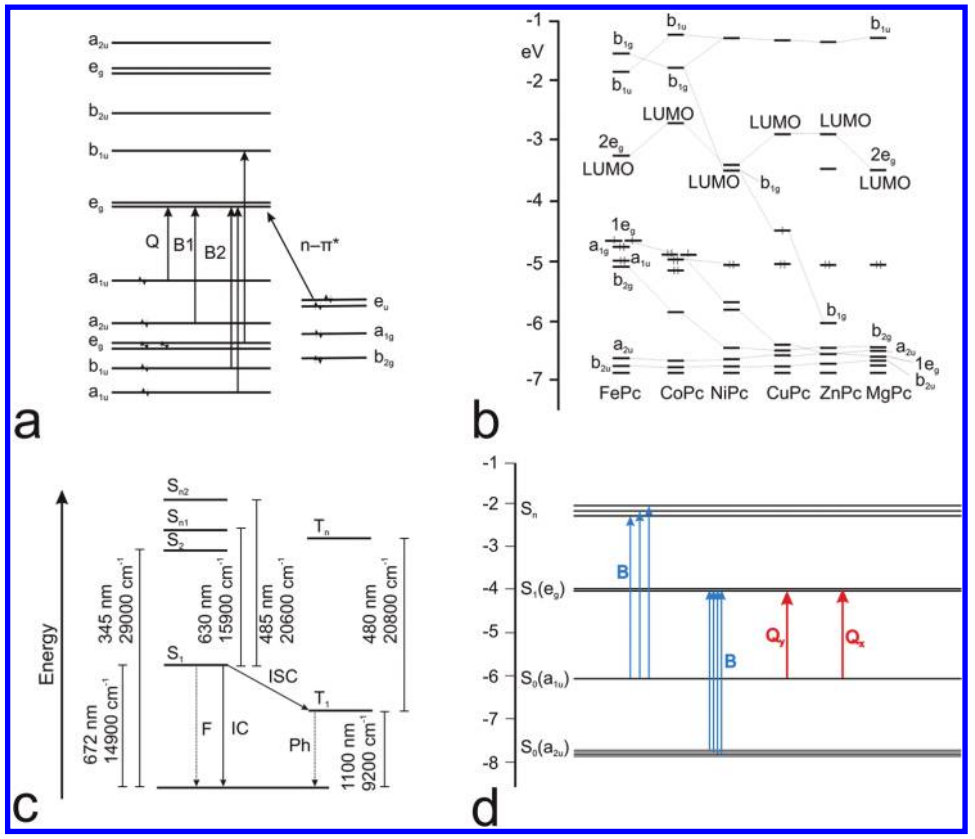

$\Delta A(t)$ presented in the previous section, we need to understand the details of the electronic transitions in phthalocyanines that are induced and probed by the laser pulses in the pump–probe experiments. Scheme 3 shows the molecular orbitals in selected phthalocyanines according to the calculations from the literature[39,58−60] and Kohn–Sham orbitals from our TD DFT calculations (Scheme 3d).

One can see from the Schemes 2 and 3 that the pump pulse at 677 nm excites the $S_0(a_{1u}) \rightarrow S_1(e_g)$ transition. The pump pulse at 360 nm can excite either of the higher excited electronic states in the $S_0(a_{1u}) \rightarrow S_n(b_{1u})$ transition and the $S_0(a_{2u}) \rightarrow S_1(e_g)$ transition (a maximum at 350 nm for $AlPcS_4$ in water and 360 nm in DMSO). Thus, probing with various spectral components in the visible range makes possible recording of the transient absorption and allows monitoring pf the repopulation of the excited states.

The previous molecular orbitals picture (Scheme 3a) based on the Schaffer, Gouterman, and Davidson considerations[58,60] suggests that the 360 nm promotes the $S_0(a_{2u}) \rightarrow S_1(e_g)$ transition (B1) and B2 transitions rather than $S_0(a_{1u}) \rightarrow S_n$ transitions to higher excited states. In contrast, the $S_0(a_{1u}) \rightarrow S_n$ transitions have been suggested recently[39] to be dominant contribution in ZnPc.

Our TD DFT calculations for $AlPcS_4$ (Table 1 and Figure 3d) show that the oscillator strengths for the $S_0(a_{1u}) \rightarrow S_1(e_g)$ (Q transition) are $f = 0.3830$ (Q_y) and 0.3859 (Q_x). For the $S_0(a_{2u}) \rightarrow S_1(e_g)$ transition, the oscillator strength is $f = 0.1452$. The B band consists of a few transitions from lower lying orbitals of the ground state to $S_1(e_g)$ with f up to 0.3041 (all transitions are gathered in Table 1). However, the transitions to the second excited state $S_0(a_{1u}) \rightarrow S_2(b_{1u})$ and to higher excited states $S_0(a_{1u}) \rightarrow S_n$ have similar oscillator strengths. Thus, the B band originates both from the inner molecular orbitals to the first excited state $S_1(e_g)$ and from the HOMO orbital $S_0(a_{1u})$ to the second excited state $S_2(b_{1u})$ as well as to higher excited states S_n. It indicates that the pump pulse at 360 nm excites both the first excited electronic state in the $S_0(a_{2u}) \rightarrow S_1(e_g)$ transition and the higher excited states in the $S_0(a_{1u}) \rightarrow S_2(b_{1u})$ and the $S_0(a_{1u}) \rightarrow S_n$ transitions. The energy difference between S_n and S_2 is only 1033 cm^{-1}. Although much higher than the thermal energy kT, the energy separation corresponds to the vibrational energy. Thus, the nonradiative energy dissipation may occur via energy relaxation between the vibrational states.

The TD DFT results presented so far determine interpretation of electronic dynamics obtained from our time resolved experimental data. Indeed, the $S_0(a_{2u}) \rightarrow S_1(e_g)$ transition pumped by 360 nm promotes the molecules to the same state as pumping at 677 nm for the $S_0(a_{1u}) \rightarrow S_1(e_g)$ transition. Therefore, both pumping wavelengths should demonstrate similar electronic dynamics of $AlPcS_4$. In contrast, the $S_0(a_{1u}) \rightarrow S_n$ transition pumped by 360 nm should result in different dynamics than that observed for the $S_0(a_{1u}) \rightarrow S_1(e_g)$ transition pumped by 677 nm.

The picture that emerges from the results presented in the paper is the following. The dynamics of $AlPcS_4$ reveals four different time scales with the time constants of 115–500 fs, 2–12 ps, and 150–500 ps. The fast femtosecond component has been also reported in the literature.[39,59,61] Savolainen et al.[39] have assigned the shortest time constant to inertial response of solvation. Fournier et al.[61] have assigned a constant of <210 fs observed in NiPc and in CuPc to the lifetime $S_2 \rightarrow S_1$ internal conversion. Rao et al.[41] have assigned the time constant < 170 fs

Table 1. Calculated Excitation Energies, Oscillator Strengths $f > 0.1$, Kohn−Sham Orbital Contributions to Transitions, and the Largest Coefficients of CI Expansion

	E, eV	λ, nm	f^a	contributions^b	coefficient
$AlPcS_4$	1.9875	623.81	0.3830	219 → 229	0.10580
				221 → 229	0.11607
				222 → 229	0.10862
				227(HOMO) → 228 (LUMO) ($S_0(a_{1u})$ → $S_1(e_g)$)	0.59031
				227(HOMO) → 229 ($S_0(a_{1u})$ → $S_1(e_g)$)	0.12058
	1.9949	621.50	0.3859	219 → 228	0.10102
				221 → 228	0.12107
				222 → 228	0.12827
				227(HOMO) → 228 ($S_0(a_{1u})$ → $S_1(e_g)$)	0.12001
				227(HOMO) → 229 ($S_0(a_{1u})$ → $S_1(e_g)$)	0.59097
	3.5054	353.69	0.1452	218 → 229	0.11303
				219 → 229	0.35226
				220 → 228	0.10412
				220 → 229	0.20897
				221 → 229	0.42233
				222 → 229	0.10918
				223 → 228	0.14080
				224 → 229	0.12435
				226 → 229 ($S_0(a_{2u})$ → $S_1(e_g)$)	0.12200
				227(HOMO) → 231 ($S_0(a_{1u})$ → S_n)	0.10268
	3.5201	352.21	0.1332	219 → 228	0.12967
				220 → 228	0.13796
				221 → 228	0.13288
				221 → 229	0.12931
				222 → 228	0.25215
				223 → 229	0.11626
				227(HOMO) → 230 ($S_0(a_{1u})$ → S_n)	0.18964
				227(HOMO) → 231 ($S_0(a_{1u})$ → S_n)	0.46735
	3.5488	349.37	0.3041	215 → 228	0.14721
				219 → 229	0.12782
				220 → 228	0.25495
				220 → 229	0.25545
				221 → 228	0.32581
				221 → 229	0.10732
				222 → 228	0.19750
				222 → 229	0.13936
				227(HOMO) → 230 ($S_0(a_{1u})$ → S_n)	0.14420
				227(HOMO) → 232 ($S_0(a_{1u})$ → S_n)	0.20454
	3.6569	339.04	0.2948	213 → 228	0.26536
				214 → 229	0.19537
				215 → 229	0.10117
				218 → 229	0.13844
				219 → 229	0.36646
				220 → 228	0.15522
				221 → 229	0.24452
				222 → 229	0.17421
				227(HOMO) → 232 ($S_0(a_{1u})$ → S_n)	0.10975
	3.9651	312.69	0.1932	211 → 229	0.12158
				212 → 229	0.13335
				213 → 228	0.36666
				213 → 229	0.39653
				216 → 228	0.13379
				219 → 228	0.11170
				227(HOMO) → 234 ($S_0(a_{1u})$ → S_n)	0.11170
	3.9731	312.06	0.1375	211 → 228	0.14594
				212 → 228	0.17506
				213 → 228	0.37033
				213 → 229	0.37569
				216 → 229	0.11856
				219 → 229	0.10609

^{a}Oscillator strength. ^{b}Orbital number.

to phase relaxation of S_n states. Our results demonstrate that the fast femtosecond component is not related to the solvation dynamics as the time constants are almost identical in both solvents, water and DMSO. We have obtained results showing that the initial decays of the signal at 500 nm are monoexponential and can be fitted with a time constant of 244 ± 98 fs in water and 155 ± 51 fs in DMSO. The initial decays of the signal at 572 nm are monoexponential and can be fitted with a time constant of 560 ± 94 fs in water and 480 ± 384 fs in DMSO. The recovery of the bleach in water at 752 nm is found to be biexponential and is fitted with time constants of 490 ± 70 fs and 3.79 ± 1.25 ps for pumping with 677 nm and 480 ± 60 fs and 2.33 ± 0.81 ps for pumping with 360 nm. It indicates that the fast femtosecond component does not depend on solvent. Thus, we find it unlikely to assign it to inertial response of solvation. We have assigned the femto second component to vibrational wavepacket dynamics of higher electronic states of $AlPcS_4$ immediately upon excitation.

The time components in the range of 2−25 ps obtained for $AlPcS_4$ at different wavelengths are similar to those reported in the literature for many phthalocyanines.[23,39,59] Savolainen et al.[39] have assigned the time constant of 2.5 ps to dielectric response of solvation. Rao et al.[41] have assigned the time constant of 3−5 ps to vibrational relaxation. Howe and Zhang[23] have assigned the time constant of 10 ps to the lifetime for the $S_2 \rightarrow S_1$ internal conversion, which seems rather long. The sudden rise at 572 nm followed by a decay (Figure 6a) is found to be biexponential and is fitted with time constants of 3.51 ± 0.50 and 220 ± 25 ps in water and 3.44 and 115 ± 95 ps in DMSO, indicating that the signals observed in the range of 500−572 nm demonstrate similar features of dynamics in both solvents. If dielectric response of solvation governed the dynamics of $AlPcS_4$, high dielectric constant solvents such as water (ε = 80) and DMSO (ε = 48) would produce distinctive features of dynamics in contrast to the obtained results. Thus, we have assigned the time constants in the range of 2−25 ps observed in our results to vibrational relaxation.

The longest time constants in the range of 150−500 ps have been assigned to the decay from S_1 to the ground state, as suggested by Howe and Zhang, because we have found dynamics occurring on a similar time scale as that in ref 23. We have found for $AlPcS_4$ in water time constants of 469 and 299 ps for the decay of the positive signals (ESA) at 500 nm for pumping at 677 and 360 nm, respectively. Therefore, we have assigned them to the decay from S_1 to the ground state. We have found no evidence of the nanosecond component in the

dynamics at 500 and 572 nm, in contrast to the results of Savolainen et al.[39] who obtained the component of 7 ns for ZnPc at 480 nm.

CONCLUSIONS

The excited state dynamics of $AlPcS_4$ have been studied in both aqueous and organic (DMSO) solutions by fluorescence and pump−probe transient absorption laser spectroscopy, providing information about the events occurring o n time scales ranging from femtoseconds to nanoseconds. The dynamics in both solvents is dominated primarily by monomeric molecules up to very high concentrations of 10^{-3} M. We have found that the fast dynamics of $AlPcS_4$ in water and DMSO reveals three time scales, 115−500 fs, 2−25 ps, and 150−500 ps. The shortest time constants have been assigned to vibrational wavepacket dynamics, the few picosecond component has been assigned to vibrational relaxation in the excited electronic states, and the 150−500 ps components represent the decay from S_1 to the ground state. The experimental and theoretical treatment proposed in this paper provides a basis for a substantial revision of the commonly accepted interpretation of the Soret transition (B transition) that exists in the literature. The Soret band in the UV absorption spectrum of phthalocyanines originates both from the electronic transitions from the inner molecular orbitals to the first excited state $S_1(e_g)$ and from the HOMO orbital $S_0(a_{1u})$ to the second excited state $S_2(b_{1u})$ as well as to higher excited states S_n.

AUTHOR INFORMATION

Corresponding Author

*E mail: abramczy@mitr.p.lodz.pl.

Notes

The authors declare no competing financial interest.

ACKNOWLEDGMENTS

The research work has been financed from funds for science in 2010−2012 as a research project "Preparation and implemen tation of new fields of studies in response to the needs of a contemporary labour market and requirements of knowledge based economy" UDA POKL.04.01.01. 00 213 /08 00 and NCN Grant Nr 3845/B/T02/2009/37.

REFERENCES

(1) Dolmans, D. E.; Fukumura, D.; Rakesh, K. *Nat. Rev. Cancer* **2003**, *3*, 380−387.
(2) Vrouenraets, M. B.; Visser, G. W. M.; Snow, G. B.; van Dongen, G. A. M. S. *Anticancer Res.* **2003**, *23*, 505−522.
(3) Henderson, B. W.; Dougherty, T. J. *Photochem. Photobiol.* **1992**, *55*, 145−57.
(4) Boyle, R. W.; Dolphin, D. *Photochem. Photobiol.* **1996**, *64*, 469−485.
(5) Brown, S. B.; Brown, E. A.; Walker, I. *Lancet Oncol.* **2004**, *5*, 497−508.
(6) Wang, X. L.; Wang, H. W.; Yuan, K. H.; Li, F. L.; Huang, Z. *Photochem. Photobiol. Sci.* **2011**, *10*, 704−711.
(7) Maduray, K.; Karsten, A.; Odhav, B.; Nyokong, T. *J. Photochem. Photobiol., B* **2011**, *103* (2), 98−104.
(8) Lui, H.; Anderson, R. R. *Arch. Dermatol.* **1992**, *128* (12), 1631−1636.
(9) Stuchinskaya, T.; Moreno, M.; Cook, M. C.; Edwards, D. R.; Russell, D. A. *Photochem. Photobiol. Sci.* **2011**, *10*, 822−831.
(10) Whitacre, C. M.; Satoh, T. H.; Xue, L.; Gordon, N. H.; Oleinick, N. L. *Cancer Lett.* **2002**, *179* (1), 43−49.
(11) Moura, V.; Lacerda, M.; Figueiredo, P.; Corvo, M. L.; Cruz, M. E. M.; Soares, R.; Pedroso de Lima, M. C.; Simões, S.; Moreira, J. N. *Breast Cancer Res. Treat.* **2011**, PMID: 21805188.
(12) Witjes, M. J.; Speelman, O. C.; Nikkels, P. G.; Nooren, C. A.; Nauta, J. M.; van der Holt, B.; van Leengoed, H. L.; Star, W. M.; Roodenburg, J. L. *Br. J. Cancer* **1996**, *73* (5), 573−580.
(13) Austwick, M.; Woodhams, J. H.; Chalau, V.; Mosse, C. A.; Eliot, C.; Lovat, L. B.; MacRobert, A. J.; Bigio, I. J.; Bown, S. G. *J. Innovative Opt. Health Sci.* **2011**, *97*, 111.
(14) Rosenkranz, A. A.; Jans, D. A.; Sobolev, A. S. *Immunol. Cell Biol.* **2000**, *78*, 452−464.
(15) Dini, D.; Hanack, M. *J. Porphyrins Phthalocyanines* **2004**, *8*, 915.
(16) Tokumaru, K.*Phthalocyanines*; Shirai, H., Kobayashi, N., Edf; IPCL Tokyo, 1997; p 170.
(17) Prasad, D. R.; Ferraudi, G. *Inorg. Chem.* **1982**, *21*, 2967.
(18) Muralidharan, S.; Ferraudi, G. *J. Phys. Chem.* **1983**, *87*, 4877.
(19) Ferraudi, G.; Muralidharan, S. *Inorg. Chem.* **1983**, *22*, 1369.
(20) Kaneko, Y.; Arai, T.; Sakarugi, H.; Tokumaru, K.; Pac, C. *J. Photochem. Photobiol., A* **1996**, *97*, 155.
(21) Kaneko, Y.; Nishimura, Y.; Arai, T.; Sakuragi, H.; Tokumaru, K.; Matsunaga, D. *J. Photochem. Photobiol., A* **1995**, *89*, 37.
(22) Kaneko, Y.; Nishimura, Y.; Takane, N.; Arai, T.; Sakuragi, H.; Tokumaru, K.; Kobayashi, N.; Matsunaga, D. *J. Photochem. Photobiol., A* **1997**, *106*, 177.
(23) Howe, I.; Zhang, J. Z. *J. Phys. Chem. A* **1997**, *101*, 3207.
(24) Ruckmann, I.; Zeug, A.; Herter, R.; Roder, B. *Photochem. Photobiol.* **1997**, *66*, 576.
(25) Chahraoui, D.; Valet, P.; Kossanyi, J. *Res. Chem. Intermed.* **1992**, *17*, 219.
(26) Kobayashi, N.; Ashida, T.; Osa, T. *Chem. Lett.* **1992**, *10*, 2031−2031.
(27) Kobayashi, N.; Lever, A. B. P. *J. Am. Chem. Soc.* **1987**, *109*, 7433.
(28) Kobayashi, N.; Lam, H.; Nevin, W. A.; Leznoff, C. C.; Koyama, T.; Monden, A.; Shirai, H. *J. Am. Chem. Soc.* **1994**, *116*, 879.
(29) Kobayashi, N.; Togashi, M.; Osa, T.; Ishii, K.; Yamauchi, S.; Hino, H. *J. Am. Chem. Soc.* **1996**, *118*, 1073.
(30) Zhong, Q.; Wang, Z.; Liu, Y.; Zhu, Q.; Kong, F. *J. Chem. Phys.* **1996**, *105*, 5377.
(31) Strickler, S. J.; Berg, R. A. *J. Chem. Phys.* **1962**, *37*, 814.
(32) Gilbert, A.; Baggott, J. *Essentials of Molecular Photochemistry*; Blackwell: Oxford, U.K., 1991; p 98.
(33) Rosenthal, I.; Krishna, C. M.; Riesz, P.; Ben Hur, E. *Radiat. Res.* **1989**, *107*, 136.
(34) Tokumaru, K. *J. Porphyrins Phthalocyanines* **2001**, *5*, 77.
(35) FitzGerald, S.; Farren, C.; Stanley, C. F.; Beeby, A.; Bryce, M. R. *Photochem. Photobiol. Sci.* **2002**, *1*, 581−587.
(36) Brożek Płuska, B.; Jarota, A.; Kurczewski, K.; Abramczyk, H. *J. Mol. Struct.* **2009**, *924−926*, 338−334.
(37) Brożek Płuska, B.; Czajkowski, W.; Kurczewska, M.; Abramczyk, H. *J. Mol. Liq.* **2008**, *141*, 140−144.
(38) Abramczyk, H.; Brożek Płuska, B.; Kurczewski, K.; Kurczewska, M.; Szymczyk, I.; Krzyczmonik, P.; Błaszczyk, T.; Scholl, H.; Czajkowski, W. *J. Phys. Chem. A* **2006**, *110* (28), 8627−8636.
(39) Savolainen, J.; van der Linden, D.; Dijkhuizen, N.; Herek, J. L. *J. Photochem. Photobiol., A* **2008**, *196*, 99−105.
(40) Ho, Z. Z.; Peyghambarian, N. *Chem. Phys. Lett.* **1988**, *148*, 107−111.
(41) Rao, S. V.; Rao, D. N. *J. Porphyrins Phthalocyanines* **2002**, *6*, 233−237.
(42) Hosokawa, Y.; Yashiro, M.; Asahi, T.; Fukumura, H.; Masuhara, H. *Appl. Surf. Sci.* **2000**, *154−155*, 192−195.
(43) Ma, G.; He, J.; Kang, C.; Tang, S. *Chem. Phys. Lett.* **2003**, 293−299.
(44) Hush, N. S.; Woolsey, I. S. *Mol. Phys.* **1971**, *21*, 465−474.
(45) Kobayashi, N.; Lever, A. B. P. *J. Am. Chem. Soc.* **1987**, *109*, 7433.
(46) Kane, A. R.; Sullivan, J. F.; Kenny, D. H.; Kenney, M. E. *Inorg. Chem.* **1970**, *9*, 1445−1448.
(47) Dhami, S.; Cosa, J. J.; Bishop, S. M.; Phillips, D. *Langmuir* **1996**, *12*, 293.

(48) Ostler, R. B. An Investigation of Intracellular PDT Mechanisms. Ph.D. Thesis, University of London. 1997.
(49) Liu, Y.; Shigara, K.; Hara, M.; Yamada, A. *J. Am. Chem. Soc.* **1992**, *113*, 440−443.
(50) Ford, W. E.; Rihter, B. D.; Kenney, M. E.; Rodgers, M. A. *J. Photochem. Photobiol.* **1989**, *50*, 277.
(51) Abramczyk, H.; Szymczyk, I. *J. Pure Appl. Chem.* **2004**, *76*, 183−187.
(52) Abramczyk, H.; Szymczyk, I. *J. Mol. Liq.* **2004**, *110*, 51−56.
(53) Abramczyk, H.; Szymczyk, I.; Waliszewska, G.; Lebioda, A. *J. Phys. Chem. A* **2004**, *108*, 264−274.
(54) Jarota, A.; Brozek Pluska, B.; Czajkowski, W.; Abramczyk, H. *J. Phys. Chem. C* **2011**, *115* (50), 24920−24930.
(55) Frisch, M. J.; Trucks, G. W.; Schlegel, H. B.; Scuseria, G. E.; Robb, M. A.; Cheeseman, J. R.; Montgomery, J. A.; Vreven, T.; Kudin, K. N.; Burant, J. C. et al. *Gaussian 03*; Gaussian Inc., Pittsburgh, PA, 2003.
(56) Harriman, A.; Richoux, M. *J. Photochem.* **1980**, *14*, 253.
(57) Oddos Marcel, L.; Madeore, F.; Bock, A.; Neher, D.; Ferencz, A.; Rengel, H.; Wegner, G.; Kryschi, C.; Trommsdorff, H. P. *J. Phys. Chem.* **1996**, *100*, 11850.
(58) Schaffer, A. M.; Gouterman, M.; Davidson, E. R. *Theor. Chim. Acta* **1973**, *30*, 9.
(59) Liao, M. S.; Scheiner, S. *J. Chem. Phys.* **2001**, *114*, 9780.
(60) Mack, J.; Stillman, M. J. *J. Am. Chem. Soc.* **1994**, *116*, 1292−1304.
(61) Fournier, M.; Pepin, C.; Houde, D.; Ouellet, R.; van Lier, J. E. *Photochem. Photobiol. Sci.* **2004**, *3*, 120.